Geochemistry Geophysics Geosystems G3
AN ELECTRONIC JOURNAL OF THE EARTH SCIENCES
Published by AGU and the Geochemical Society

Article
Volume 8, Number 9
21 September 2007
Q09012, doi:10.1029/2006GC001503
ISSN: 1525-2027

Oxygen-isotope and trace element constraints on the origins of silica-rich melts in the subarc mantle

J. M. Eiler
Division of Geological and Planetary Sciences, California Institute of Technology, MC 100-23, Pasadena, California 91125, USA (eiler@gps.caltech.edu)

P. Schiano
Departement des Sciences de la Terra (UMR 6524 "Magmas et Volcans"), Université Blaise Pascal, 5 Rue Kessler, F-63038 Clermont-Ferrand Cedex, France

J. W. Valley and N. T. Kita
Department of Geology, University of Wisconsin, Madison, Wisconsin 53706, USA

E. M. Stolper
Division of Geological and Planetary Sciences, California Institute of Technology, MC 100-23, Pasadena, California 91125, USA

[1] Peridotitic xenoliths in basaltic andesites from Batan island in the Luzon arc contain silica-rich (broadly dacitic) hydrous melt inclusions that were likely trapped when these rocks were within the upper mantle wedge underlying the arc. These melt inclusions have been previously interpreted to be slab-derived melts. We tested this hypothesis by analyzing the oxygen isotope compositions of these inclusions with an ion microprobe. The melt inclusions from Batan xenoliths have $\delta^{18}O_{VSMOW}$ values of 6.45 ± 0.51‰. These values are consistent with the melts having been in oxygen isotope exchange equilibrium with average mantle peridotite at temperatures of $\geq$875°C. We suggest the $\delta^{18}O$ values of Batan inclusions, as well as their major and trace element compositions, can be explained if they are low-degree melts (or differentiation products of such melts) of peridotites in the mantle wedge that had previously undergone extensive melt extraction followed by metasomatism by small amounts (several percent or less) of slab-derived components. A model based on the trace element contents of Batan inclusions suggests that this metasomatic agent was an aqueous fluid extracted from subducted basalts and had many characteristics similar to slab-derived components of the sources of arc-related basalts at Batan and elsewhere. Batan inclusions bear similarities to ''adakites,'' a class of arc-related lava widely considered to be slab-derived melts. Our results suggest the alternative interpretation that at least some adakite-like liquids might be generated from low-degree melting of metasomatized peridotites.

Components: 14,199 words, 6 figures, 2 tables.

Keywords: subduction zone; slab melting; oxygen isotopes; adakites.

Index Terms: 1031 Geochemistry: Subduction zone processes (3060, 3613, 8170, 8413); 1037 Geochemistry: Magma genesis and partial melting (3619); 1041 Geochemistry: Stable isotope geochemistry (0454, 4870).

Received 9 October 2006; **Revised** 12 June 2007; **Accepted** 19 June 2007; **Published** 21 September 2007.

Eiler, J. M., P. Schiano, J. W. Valley, N. T. Kita, and E. M. Stolper (2007), Oxygen-isotope and trace element constraints on the origins of silica-rich melts in the subarc mantle, *Geochem. Geophys. Geosyst.*, *8*, Q09012, doi:10.1029/2006GC001503.

1. Introduction

[2] Convergent margin magmatism is thought to be dominated by partial melting of peridotitic mantle wedge in response to influxes of aqueous fluids and/or hydrous melts released from subducting lithosphere [*Gill*, 1981; *Tatsumi et al.*, 1983; *Davies and Bickle*, 1991; *McCulloch and Gamble*, 1991; *Davies and Stevenson*, 1992]. In this process, slab-derived metasomatic agents control the budgets of many minor and trace elements in the mantle wedge [*Plank and Langmuir*, 1993; *Elliott et al.*, 1997] and strongly influence its melting properties and rheology [*Kushiro et al.*, 1968; *Stolper and Newman*, 1994; *Billen and Gurnis*, 2001; *Hirth and Kohlstedt*, 2003; *Baker et al.*, 2005], but they comprise only a small mass fraction (∼1–2% or less [*Eiler et al.*, 2000, 2005]) of the sources of most arc magmas.

[3] Despite their dominantly peridotitic sources, arc volcanoes erupt larger fractions of relatively silica-rich lavas (e.g., basaltic andesites, andesites, dacites and rhyolites) than volcanic centers in other environments (e.g., ocean ridges, plateaus and islands [*Gill*, 1981]). The major element compositions of most silica-rich arc lavas are attributable to crustal differentiation of more mafic magmas [*Davidson*, 1996]. However, a variety of other processes contribute to these silica-rich compositions, including partial melting of basaltic material in subducting slabs and/or reaction between such melts and peridotites in the mantle wedge [*Ringwood and Green*, 1966; *Condie and Swenson*, 1973; *Ringwood*, 1974; *Kay*, 1978; *Martin*, 1986, 1988; *Defant and Drummond*, 1990; *Rapp et al.*, 1991; *Martin et al.*, 2005]; partial melting of mafic rocks deep in the crust of the overriding plate [*Atherton and Petford*, 1993]; differentiation of basaltic melt in the upper mantle [*Kelemen*, 1990; *Macpherson et al.*, 2006]; or low-degree (∼1–2%) partial melting of peridotites in the presence of water [*Baker et al.*, 1995; *Gaetani and Grove*, 1998, 2003; *Hirschmann et al.*, 1998, 1999]. Resolving the relative importance of these processes for explaining the silica-rich character of arc lavas has implications for the thermal and dynamical evolution of subducting slabs [*Peacock*, 2003; *Kelemen et al.*, 2003a], for the chemical budgets of arc magmatism [*Plank and Langmuir*, 1993; *Elliott et al.*, 1997], for the mechanisms responsible for growth of the continental crust [*Rudnick and Fountain*, 1995; *Wang et al.*, 2003], and for the composition of deeply subducted lithosphere [*Kelley et al.*, 2005].

[4] "Adakites," magmatic rocks with unusually low Y contents (generally less than 20 ppm) and high Sr/Y ratios (generally greater than 50), have been suggested to have a special significance for our understanding of silica-rich arc magmas [*Defant and Drummond*, 1990]. Archetypical adakites are dacites from convergent margins where relatively young ocean lithosphere has been subducted (although the rock name has been applied to other rock types and settings). It has been suggested that adakites are among the clearest examples of arc-related melts that form by partial melting of basaltic components of subducted ocean lithosphere [*Defant and Drummond*, 1990; *Rapp et al.*, 1991]. This hypothesis is supported by the facts that partial melts of eclogite are broadly dacitic over a significant range in melt fraction [*Rapp et al.*, 1991] and leave garnet-rich residues that retain Y and heavy-rare earth elements, promoting low Y and high Sr/Y. Alternatively, mirroring the debate about silica-rich arc lavas generally, it has also been suggested that adakites form by high-pressure crystallization-differentiation of basalt [*Macpherson et al.*, 2006] or by melting garnet- and/or amphibole-rich crystal cumulates near the base of thick crust [*Chung et al.*, 2003; *Wang et al.*, 2005]. Both processes involve melt/garnet fractionation and produce broadly dacitic melt and so can also explain the critical features of adakites. This debate also touches on the origin of high-Mg andesites, many of which have the trace element characteristics of adakites and have been suggested to form by reaction of slab-derived melts with mantle peridotites [*Green and Ringwood*, 1967; *Kay*, 1978; *Kelemen*, 1995; *Yogodzinski and Kelemen*, 1998]. Alternatively, high-Mg andesites may be direct partial melts of hydrous peridotites [*Tatsumi*, 1981, 1982; *O'Nions and McKenzie*, 1988; *Grove et al.*, 2002].

[5] Melt inclusions (now glass) from metasomatized xenoliths from Mount Iraya on the island of Batan (northern-most Philippines; a part of the Luzon-Taiwan volcanic arc) are a well-documented example of silica-rich melts in a convergent margin [*Richard et al.*, 1986; *Vidal et al.*, 1989; *Maury et al.*, 1992; *Schiano et al.*, 1995]. These peridotitic xenoliths are hosted by basaltic andesite and are believed to sample the upper portions of the mantle wedge beneath the Luzon arc. The melt inclusions contained in these xenoliths have silica contents up to ~63% and Sr/Y ratios up to ~250, within the adakitic range. The melt inclusions correspond to one end-member of the array of compositions of basaltic andesites from Batan (Figure 1) [*Schiano et al.*, 1995], and thus they could have bearing on the petrogenesis of the lavas that carried the xenoliths to the surface. These melt inclusions clearly existed in the mantle and so cannot be products of differentiation in or partial melting of the arc crust (though they could be products of differentiation of basalt in the mantle wedge [*Macpherson et al.*, 2006]); and their low MgO contents (0.5–1.7 wt.% [*Schiano et al.*, 1995]) (Table S3 in the auxiliary material[1] to this paper) are within a range that has been previously suggested to preclude reaction between slab-derived melts and mantle peridotites [*Rapp et al.*, 1999] (although they could also reflect modification of peridotite-equilibrated melts by crystallization of olivine and other phases). These inclusions have been interpreted as partial melts of basalts in the subducted South China Sea slab [*Schiano et al.*, 1995], and they have been cited as evidence that adakites can be generated by melting of subducted crust and can pass through the mantle wedge without extensive reaction with peridotite [*Martin et al.*, 2005, and references therein]. If these interpretations are correct, Batan melt inclusions could provide valuable information on the role of slab melting in the petrogenesis of arc-derived magmas, especially those that are relatively silica-rich. Note, however, that the Batan melt inclusions have major element characteristics (other than MgO and Mg/Fe ratio, which can be disturbed by crystallization) similar to those suggested for very low degree (approximately ≤1–2%) partial melts of peridotite at low pressure (<1.5 GPa [*Baker et al.*, 1995; *Hirschmann et al.*, 1998]). Moreover, *McDermott et al.* [1993] suggested that the trace element characteristics of Batan lavas (and, by extension, compositionally similar Batan melt inclusions) could be generated by melting peridotite that had been metasomatized by slab-derived fluid. Here, we use oxygen isotopes to constrain further the origins of Batan inclusions.

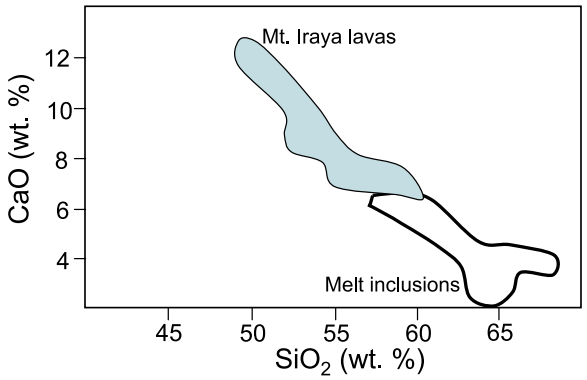

Figure 1. Geochemical trend defined by Batan melt inclusions (unfilled field) and host Mt. Iraya lavas (gray field). These data are consistent with Batan inclusions being a mixing end-member of magmas parental to Mt. Iraya lavas or being products of a petrogenetic process related to that responsible for generating Mt. Iraya lavas. Data are from *Richard et al.* [1986], *McDermott et al.* [1993], and *Schiano et al.* [1995].

[6] Mantle peridotites typically have $\delta^{18}O_{VSMOW}$ values of approximately 5.5 ± 0.2‰ [*Mattey et al.*, 1994] (see *Eiler et al.* [1996] and *Ducea et al.* [2002] for exceptions). In contrast, the major components of the upper ~10 km of the ocean lithosphere typically have $\delta^{18}O_{VSMOW}$ values in the following ranges [*Kolodny and Epstein*, 1976; *Arthur et al.*, 1983; *Gregory and Taylor*, 1981; *Alt et al.*, 1986; *Staudigel et al.*, 1995]: opaline oozes, 35–42‰; carbonate oozes, 25–32‰; pelagic clays, 15–25‰; terrigenous and volcaniclastic sediments, and basalts and diabases subjected to weathering and low-temperature hydrothermal alteration (i.e., layer-2 ocean crust), 7–15‰; and gabbros subjected to high-temperature hydrothermal alteration (i.e., layer-3 ocean crust), 0–6‰. Importantly, all of these materials have broadly similar oxygen concentrations, and so $\delta^{18}O$ values of mixtures between these components are approximately linear functions of the mass fractions of the end-members. It is also important to note that magmatic differentiation processes (partial melting and crystallization) also lead to variations in $\delta^{18}O$ [*Eiler*, 2001], and these variations must be considered before reaching conclusions regarding the

[1] Auxiliary material data sets are available at ftp://ftp.agu.org/apend/gc/2006gc001503. Other auxiliary material files are in the HTML.

oxygen isotope compositions of the sources of magmatic rocks.

2. Samples

[7] We examined inclusions and host olivine crystals from xenolith B3N, collected from a high-K basaltic andesite erupted $\leq$1.48 ka ago from Mount Iraya, Batan Island [*Schiano et al.*, 1995]. The peridotitic xenoliths in this flow are harzburgites believed to come from a depth of $\sim$30 km, near the top of the mantle wedge between the overriding Philippine plate and the subducting South China Sea plate [*Maury et al.*, 1992].

[8] Xenolith B3N is a deformed spinel harzburgite consisting of primary porphyroclasts of olivine (Fe_{90-93}), orthopyroxene (En_{90-92}) and spinel ($Mg_{0.62-0.64}Fe^{2+}_{0.36-0.38}Fe^{3+}_{0.04-0.08}Al_{0.62-0.90}Cr_{0.98-1.22}O_4$) [*Richard et al.*, 1986; *Maury et al.*, 1992; *Schiano et al.*, 1995]. Clinopyroxene is rare in this sample, suggesting that it is a fragment of the subarc mantle that is residual to high extents of melting. The sample also contains hydrous metasomatic phases (phlogopite and amphibole) and undeformed neoblasts of olivine (Fo_{78-90}) and orthopyroxene (En_{86-88}). Petrographic observations suggest that neoblastic olivine formed from recrystallization of primary olivine porphyroclasts, accompanied by variable amounts of Mg loss and Fe gain and growth of metasomatic phlogopite and amphibole [*Richard et al.*, 1986; *Maury et al.*, 1992; *Schiano et al.*, 1995]. It also seems possible that some neoblastic olivine and orthopyroxene precipitated from the same infiltrating metasomatic agent responsible for growth of hydrous metasomatic phases.

[9] Olivine porphyroclasts and neoblasts and metasomatic hydrous phases in sample B3N commonly contain inclusions. Inclusions in olivine porphyroclasts typically occur as linear trails of small (approximately $\leq$50 μm diameter) polyphase assemblages of silica-rich (SiO_2 > 57 wt.%) glass and H_2O-rich bubbles of liquid and vapor [*Schiano et al.*, 1995]. Polyphase inclusions are typically 50:50 mixtures of glass and fluid. Homogenization temperatures of these polyphase inclusions (a minimum estimate of their liquidus temperatures) average 920 $\pm$ 10°C. Neoblasts and hydrous metasomatic phases contain larger (typically 30–150 μm diameter) inclusions of either a combination of silicate glass and H_2O-rich fluid (like the inclusions in porphyroclasts) or H_2O-rich fluid alone. This suggests that both hydrous silicate melt and aqueous fluid were present during metasomatism and recrystallization [*Schiano et al.*, 1995]. These inclusions typically define crystallographic planes in their host minerals and were likely trapped from grain-boundary melts and/or fluids during growth of the neoblasts and hydrous metasomatic minerals [*Schiano et al.*, 1995]. There are no obvious compositional differences between glass inclusions in porphyroclasts and inclusions in neoblasts. We focused our analysis on inclusions in neoblasts because their larger size facilitated ion microprobe analyses of glass.

[10] Batan inclusions might have been trapped from silicate melts or might instead be exsolved from solute-rich aqueous fluids or supercritical liquids. Glass and fluid in polyphase Batan inclusions are typically subequal in volume within each inclusion and glass typically contains approximately 5 wt.% H_2O [*Schiano et al.*, 1995]. Thus, prior to phase separation, these inclusions were approximately 30 wt.% H_2O and 70 wt% silicate (assuming the trapped aqueous phase has a density of 1 g/cc and glass has a density of 2.5 g/cc). This bulk composition is too silicate rich to be an aqueous phase in equilibrium with mafic or ultramafic rock at 1 GPa; i.e., it lies on the "melt" side of the solvus between hydrous, silicate melts and aqueous fluids in these compositional systems [*Stalder et al.*, 2001; *Kessel et al.*, 2005a]. Thus these polyphase inclusions most likely quenched from H_2O-rich silicate melt, not aqueous fluid or a supercritical phase. Some glass inclusions contain crystals of sulfide, indicating that this hydrous silicate melt also contained significant amounts of sulfur.

3. Methods

[11] Major element compositions of minerals and glasses in peridotite xenolith B3N were taken from published analyses by *Schiano et al.* [1995] or were measured using a JEOL 733 electron microprobe at Caltech. These new measurements used an accelerating voltage of 15 keV, a sample current of 10 nA, a defocused beam (15–20 μm) for glasses and a focused beam for minerals. The H_2O-rich character of fluid associated with glass inclusions was established by previously published laser-Raman analyses; water contents of glasses were previously determined by SIMS [*Schiano et al.*, 1995].

[12] Oxygen-isotope analyses were made using the CAMECA IMS-1280 ion microprobe at the University of Wisconsin. Measurements were made using a primary beam of $^{133}Cs^+$ ions with a 20 keV impact energy, focused to a diameter of approxi-

mately 5–10 μm on the sample surface. Primary ion intensities were between ~1 nA and ~5 nA but were held constant for each analytical session. An electron flood gun was used for charge compensation. Secondary O^- ions were extracted, accelerated by 10 keV, and focused and collimated using a secondary optic alignment described by *Kita et al.* [2004]. The mass resolving power was ~2500, enough to separate hydride interferences on ^{18}O.

[13] The intensity of the $^{16}O^-$ secondary ion beam typically varied between 1 and 5×10^9 counts per second (cps), depending on the intensity of the primary ion beam (i.e., $\sim 10^9$ cps of secondary ions were detected per nA of primary beam current). Two Faraday cups were used to measure $^{16}O^-$ (registered through a 10^{10} Ω resistor) and $^{18}O^-$ (registered through a 10^{11} Ω resistor) simultaneously. The baseline of each amplifier was calibrated once each day; drift during the day was insignificant compared to the noise level of the detectors ($\leq$1000 cps for the circuit using the 10^{11} Ω resistor). Immediately before each analysis, any small misalignment of the secondary optics was corrected for by scanning the position of the secondary ion beam across the field aperture of the mass spectrometer to maximize its detected intensity.

[14] Each analysis consisted of 20 cycles of 4 seconds each; the internal precision of the $^{18}O/^{16}O$ ratio was typically between 0.05 and 0.15‰, 1σ (varying inversely with the secondary beam intensity). The external precision, as measured by the reproducibility of repeat analyses of nominally homogeneous standards of silicate minerals and glasses (see the auxiliary material), averaged ±0.21‰, 1 standard deviation, spot-to-spot. External precision was poorer than internal precision by a factor of 2, on average. We suspect this reflects some combination of imperfect charge neutralization of the sample surface during analysis, variations in analytical fractionation caused by moving the sample in the instrument reference frame, and/or isotopic heterogeneity of standards. In any event, we suggest the external precision of our analyses of unknowns, not considering any systematic errors in standardization (below), is ±0.2‰, 1σ.

[15] Analyses of oxygen isotope composition by SIMS typically involve an instrumental mass fractionation that varies from material to material, the so-called "matrix effect" [*Eiler et al.*, 1997]. Matrix effects stem from a variety of known causes but generally cannot be predicted on the basis of physical principles and must be corrected for empirically. Matrix effects in silicate minerals previously have been corrected for by interpolation based on major element composition; i.e., the matrix effect for an unknown material is calculated as the weighted average of those for two or more standards that, when combined in the appropriate proportions, approximate the major element composition of the unknown. The approach we follow here is as follows: Batan glass inclusions have normative compositions dominated by albite, anorthite, orthoclase, quartz and hypersthene, and they contain approximately 5 wt.% H_2O [*Schiano et al.*, 1995] (auxiliary material). We approximated the instrumental fractionation for these glasses as the weighted sum, by oxygen fraction, of those measured for albite glass, anorthite glass, orthoclase glass, silica glass and crystalline orthopyroxene (auxiliary material), in proportions equal to the anhydrous norm of the unknown glass, and then apply a correction equal to the difference between anhydrous albite glass and albite glass containing 5 wt.% H_2O. For olivines, there is no variation in instrumental fractionation with major element composition over the range relevant to our samples, so we standardized all measurements of unknown olivines by assuming an instrumental fractionation equal to that for San Carlos olivine standard. See the auxiliary material for further details and data for standards.

4. Results

[16] All oxygen isotope analyses of Batan inclusions and host olivines made as part of this study are summarized in Table 1. Seven analyses of five separate inclusions (one of which was analyzed three times; the others once each) yield an average $\delta^{18}O_{VSMOW}$ of 6.45 ± 0.51‰ (±0.19‰ 1 standard error, i.e., standard deviation divided by the square root of the number of measurements). Twenty-five analyses of three host olivine crystals yield an average $\delta^{18}O_{VSMOW}$ of 5.34 ± 0.42‰ (±0.08‰ st. err.). Each of these two populations of analyses has a standard deviation that is a factor of 2 worse than the external precision for analyses of nominally homogeneous standards. We think this difference likely reflects some combination of errors in corrections for matrix effects, analytical fractionations caused by vertical relief between the separately mounted samples and standards, and real isotopic heterogeneity of the samples. We can examine the importance of fractionations caused by sample relief by assuming that the three olivine grains that host our analyzed inclusions are identical to each other in $\delta^{18}O$ with a value equal to

Table 1. SIMS Analysis of $\delta^{18}O_{VSMOW}$ Values of Batan Inclusions and Host Olivines[a]

	B3N1			B3N2			B3N3		
	Host Olivine	Inclusion	Normalized Inclusion[b]	Host Olivine	Inclusion	Normalized Inclusion[b]	Host Olivine	Inclusion	Normalized Inclusion[b]
	5.45	5.79	5.63	5.31	6.31	6.64	5.14	6.84	6.83
	5.35	7.06	6.90	4.58	5.84	6.17	4.75		
	5.04			5.12	7.10	7.43	5.38		
	5.47			5.05	6.18	6.51	6.19		
	5.38			4.93			5.60		
	5.11			5.14			5.27		
	5.22			4.96			5.16		
	5.10								
	5.13								
	5.33								
	6.30								
	6.12								
	6.10								
	5.88								
Average	5.50	6.42	6.26	5.01	6.36	6.69	5.35	6.84	6.83
1 St.dev.	0.41	0.63	0.63	0.21	0.46	0.46	0.42	0.18[c]	0.18[c]
1 St.err.	0.11	0.45	0.45	0.08	0.23	0.23	0.16	0.18[c]	0.18[c]

[a] Overall averages: All olivines, 5.34 ± 0.42 (±0.08 st. err.); all inclusions, 6.44 ± 0.51 (±0.19 st. err.); all normalized inclusions, 6.59 ± 0.53 (±0.20 st. err.).
[b] Restandardized assuming host olivine has a $\delta^{18}O_{VSMOW}$ value of 5.34‰.
[c] Based on external precision of standard glasses.

their average measured value (a reasonable approximation, given the small range in $\delta^{18}O$ of most mantle olivines [*Eiler*, 2001]). In this case, the average value for glass changes little, to 6.59 ± 0.53 (±0.20‰ st. err) and the reproducibility for olivines (i.e., based on reproducibility within each grain) improves slightly to ±0.37‰ (±0.07‰ st. err.). The important point, however, is that regardless of these small corrections, to first order, all olivines have $\delta^{18}O$ values similar to olivine from typical mantle peridotites (~5.0–5.4‰ [*Mattey et al.*, 1994; *Eiler*, 2001]), and all glasses have $\delta^{18}O$ values of ~6.5‰.

5. Discussion

[17] The oxygen isotope compositions of Batan melt inclusions are consistent with those predicted for melts of similar major element composition in equilibrium with average mantle peridotite at temperatures of 875°C or greater (Figure 2). That is, while these inclusions are approximately 1–1.5‰ higher in $\delta^{18}O$ than typical peridotitic olivines, this difference is consistent with equilibrium oxygen-isotope fractionation between quartzo-feldspathic melts and typical mantle peridotite mineralogies at magmatic temperatures [*Eiler*, 2001, and references therein]. This result also suggests that Batan melt inclusions contain little or no oxygen from sources rich in weathered, hydrothermally altered or authigenic phases, such as basaltic, gabbroic and metasedimentary materials in a subducted slab. Instead, our data are consistent with the interpretation that Batan siliceous melt inclusions are derived from or equilibrated with mantle peridotites having typical $\delta^{18}O$ values, or are differentiation products of more mafic melts that were derived from or in equilibrium with mantle peridotites.

[18] The oxygen isotope compositions of Batan inclusions contrast with those of melt veins and inclusions in a peridotite xenolith collected from an alkali basalt from Simberi island, Papua New Guinea [*Eiler et al.*, 1998] (Simberi is a volcano associated with the Manus-Kilinailau subduction zone). These latter glasses have $\delta^{18}O_{VSMOW}$ values up to 11.3 ± 1.3‰, consistent with derivation from a source rich in oxygen from subducted sediments and/or altered upper oceanic crust. These previous results show that metasomatic melts and/or fluids can be extracted from a subducted slab and transported through the mantle wedge without undergoing extensive oxygen-isotope exchange with the mantle peridotites through which they move. *Eiler et al.* [1998] suggested that this reflects either the fast rate of

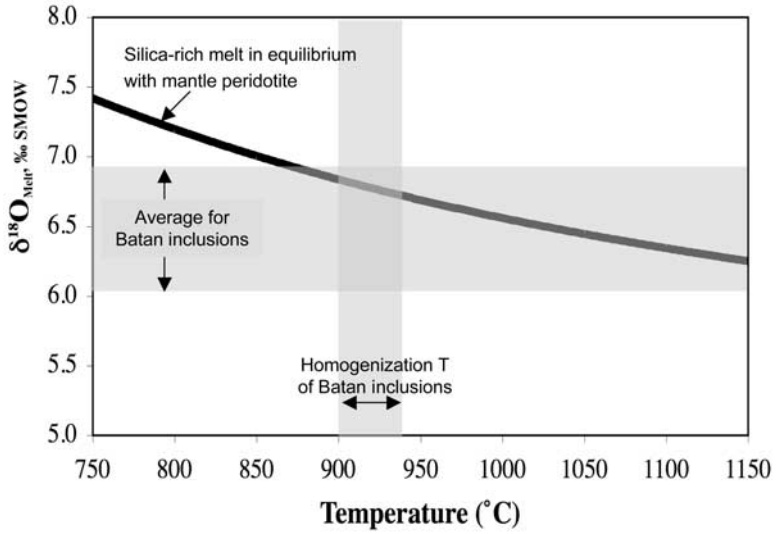

Figure 2. The heavy curve plots the $\delta^{18}O_{VSMOW}$ values of dacitic melts in oxygen-isotope exchange equilibrium with average mantle peridotite as a function of the temperature of equilibration. This calculation assumes a major element composition for silica-rich melt equal to the average measured for Batan glass inclusions [*Schiano et al.*, 1995] (Table S3 in the auxiliary material for this paper), an oxygen-isotope composition for mantle peridotite equal to the sources of average, normal mid-ocean-ridge basalts [*Eiler et al.*, 1998; *Eiler*, 2001], and oxygen-isotope fractionation factors summarized by *Eiler* [2001]. The horizontal and vertical gray bands indicate the oxygen-isotope compositions (this study) and homogenization temperatures [*Schiano et al.*, 1995], respectively, of Batan inclusions (in both cases the position and width of the band reflect the average(2 std. err.). Data presented in this study are consistent with Batan inclusions being in oxygen-isotope exchange equilibrium with typical upper mantle peridotites.

movement of slab-derived melt and/or fluid through the wedge (i.e., because diffusion-limited oxygen isotope exchange is relatively slow, even at mantle temperatures) or that slab-derived melt can move through conduits that were previously armored by metasomatic phases.

[19] The mantle-equilibrated oxygen isotopic ratios of Batan inclusions argue against involvement of several petrogenetic processes in their origins and are consistent with several others:

[20] Batan inclusions are not partial melts of weathered, hydrothermally altered or sedimentary constituents of subducted oceanic lithosphere that were transported through the mantle wedge with little or no reaction or exchange with peridotites. Similarly, Batan inclusions are not well explained as partial melts of portions of the mantle wedge that underwent extensive metasomatism (i.e., where metasomatic agent contributes tens of % of the oxygen of the hybrid source) by fluids or melts derived from ^{18}O-rich or ^{18}O-poor sections of subducted ocean crust (this was the preferred interpretation of high-$\delta^{18}O$ inclusions from Simberi island presented by *Eiler et al.* [1998]).

[21] On the other hand, Batan inclusions *could* be partial melts of parts of subducted ocean crust that fortuitously yield melts having $\delta^{18}O$ values in equilibrium with mantle peridotite (or, similarly, a combination of melts from ^{18}O-rich and ^{18}O-poor sources that fortuitously yields such $\delta^{18}O$ values [*Bindeman et al.*, 2005]). They also could be slab-derived melts that underwent extensive oxygen isotope exchange with mantle peridotites during transport through the mantle wedge. Or, they might be products of high-pressure crystallization-differentiation of normal-$\delta^{18}O$ basaltic partial melts of mantle wedge. Finally, they could be low-degree partial melts of normal-$\delta^{18}O$ mantle wedge peridotites. While it may not be possible to strictly rule out any one of these possibilities, the following sections examine their various strengths and weaknesses in explaining the full spectrum of major element, trace element and isotopic constraints on the origins of Batan inclusions.

5.1. Slab-Derived Melts That Lack Anomalous Oxygen Isotope Signatures?

[22] Oxygen isotope data are consistent with Batan inclusions being partial melts of basaltic or gabbroic components of the subducted South China

Sea slab that are in oxygen isotope equilibrium with the mantle either because their sources escaped weathering or hydrothermal alteration before subduction or because they underwent oxygen isotope exchange with the mantle wedge before or during entrapment. This hypothesis is appealing because Batan inclusions have traits often associated with slab-derived melts (e.g., elevated SiO_2 contents, low abundances of heavy rare earth elements and Y, and high Sr/Y ratios). On the other hand, normal-$\delta^{18}O$ components of old oceanic crust are unusual [*Gregory and Taylor*, 1981; *Alt et al.*, 1986; *Staudigel et al.*, 1995], and previous data for Simberi island inclusions [*Eiler et al.*, 1998] demonstrate that melts of sources rich in slab components can retain relatively dramatic oxygen-isotope anomalies, despite later transport through the mantle. Similarly, several suites of arc lavas are known to have oxygen isotope anomalies inherited from slab-derived components, despite transport through the mantle wedge [e.g., *Eiler et al.*, 2000, 2005; *Bindeman et al.*, 2005]. Thus, if Batan inclusions are slab melts, their oxygen isotope compositions contrast both with simple expectations and with previous data for subduction-zone melts.

[23] Figure 3a presents the average primitive-mantle-normalized trace element composition of Batan inclusions, based on analyses of a subset of the plotted elements in glass inclusions (circles) and analyses of a larger subset of elements in inclusion-rich olivines (diamonds; see the caption to Figure 3a for details; both sets of data from *Schiano et al.* [1995]). Note that the inclusion-rich olivines in Batan xenoliths contain sulfides, which doubtless host a large proportion of the Pb and Cu added to these xenoliths by metasomatic melt [*Schiano et al.*, 1995]. Measurements of inclusion-rich olivines will faithfully represent the bulk abundances of these elements in metasomatic melt only if all phases formed by quenching of metasomatic melt (glass, fluid, sulfide, etc.) are sampled in their correct relative proportions (i.e., preferential enrichment or depletion in sulfide could enrich or deplete olivine separates in Pb and Cu). However, repeat measurements of inclusion-rich olivines from Batan xenoliths are reproducible in their relative abundances of trace elements, and essentially indistinguishable in their Pb anomalies; so, it seems unlikely to us that selective sampling of sulfide (or any other quench phase) in the inclusion-rich olivine separates has greatly biased the estimated compositions of metasomatic melts.

[24] The most noteworthy features of the trace element compositions of Batan inclusions are: a approximately hundredfold enrichment of incompatible elements relative to compatible elements; a pronounced (approximately fivefold) positive anomaly in Pb; a large (approximately tenfold) negative anomaly in Nb; and high concentrations of Cu and Sn (despite uncertainty in the correct location of these elements on the horizontal axis in Figure 3, they likely constitute ~10x positive anomalies). Batan inclusions also have modest (factor of 2 to three) positive anomalies of U and Sr and negative anomalies of Eu and Ti.

[25] Figure 3b compares the estimated average composition of Batan inclusions from Figure 3a (filled circles) to predicted compositions of low-degree (1 wt.%) partial melts of altered ocean crust [*Bach et al.*, 2003] in the eclogite facies. These calculated slab melt compositions are based on estimated or experimentally measured garnet/melt, clinopyroxene/melt and rutile/melt distribution coefficients for the elements of interest, and an assumed residual mineralogy of 60% garnet, 40% clinopyroxene (mixed with 1% rutile for the models labeled "Kelemen-rutile" and "Xiong-rutile"). Each model corresponds to a different set of constraints on the relevant mineral-melt distribution coefficients; see the auxiliary material for a compilation and discussion of these various distribution coefficients. Models plotted with solid lines are based on direct experimental studies of eclogite melting; those plotted with dashed lines use inferred distribution coefficients based on experiments in other systems. Note that the model "Kessel" is based on experimental partitioning data between eclogite and an aqueous supercritical phase that could be described as broadly "melt-like" in its physical and chemical properties, but is not, strictly speaking, melt [*Kessel et al.*, 2005a, 2005b]. Each of these models would result in lower overall concentrations of incompatible elements and somewhat weaker element-specific anomalies for higher degrees of melting; otherwise, the patterns of relative trace element concentrations are insensitive to variations in degree of melting. For this reason, our discussion focuses on the shape, not position, of model results in Figure 3b. We do not consider partial melts of subducted sediment because the Sr isotope compositions of metasomatized Batan xenoliths ($^{87}Sr/^{86}Sr$ = 0.7044 to 0.7048 [*Maury et al.*, 1992]) preclude a significant component of pelagic sediment ($^{87}Sr/^{86}Sr$ = 0.715 to 0.718 for Mesozoic and younger marine sedi-

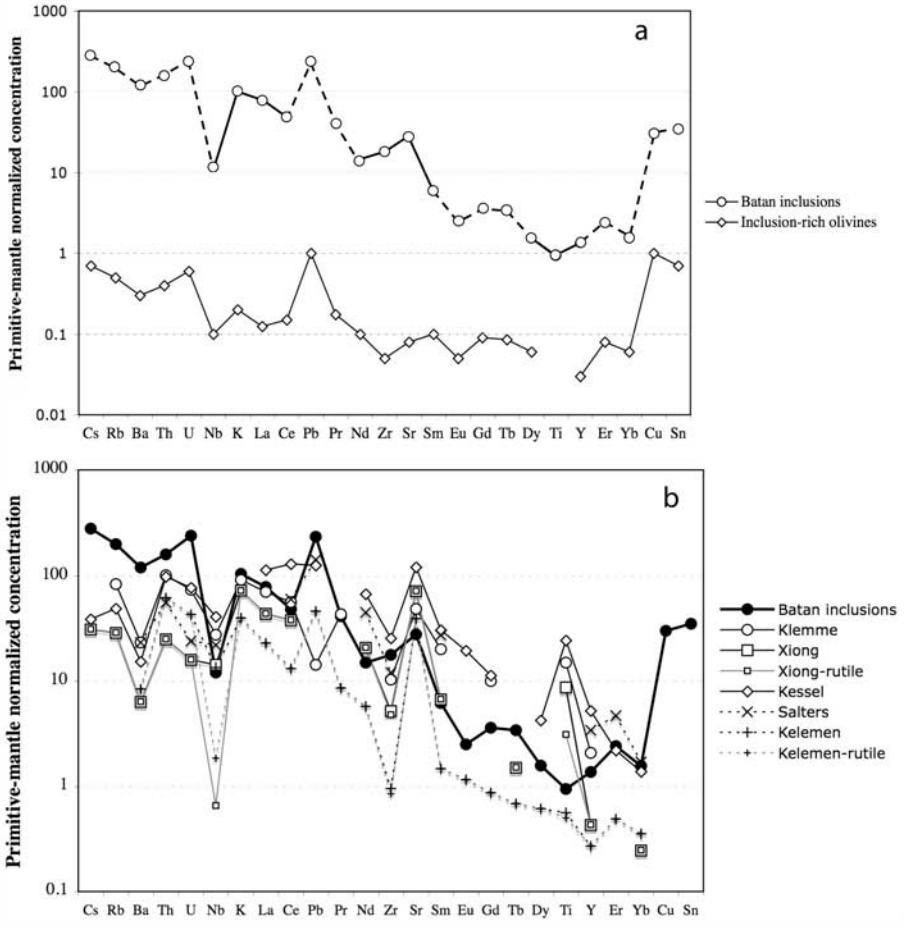

Figure 3. (a) Primitive-mantle-normalized trace element abundances in Batan inclusions and inclusion-rich olivines. The dashed portions of the line for Batan inclusions indicate inferred abundances in inclusion glass of elements that were analyzed in inclusion-rich olivines but not in inclusions alone. This estimate was made by increasing the measured trace element concentrations for inclusion-rich olivines by a multiple equal to the average measured concentration ratio for inclusions versus inclusion-rich olivines for elements of similar compatibility that were analyzed in both (i.e., Cs, Rb, Ba, Th, and U in inclusions were calculated on the basis of measurements of Nb, K, La, and Ce in inclusions and inclusion-rich olivines; Pb and Pr were calculated on the basis of data for Ce and Nd; Eu, Gd, and Tb were calculated on the basis of data for Sm and Dy; and Er, Cu, and Sn were calculated on the basis of data for Ti and the heavy-rare earths). (b) Primitive-mantle-normalized trace element abundances calculated for melts in equilibrium with altered basalt having an eclogitic mineralogy compared to the average composition of Batan inclusions (from Figure 3a). The names used to refer to each model correspond to the first authors of the publications from which the relevant distribution coefficients were taken, including *Klemme et al.* [2002], *Xiong* [2006], *Kessel et al.* [2005b], *Salters et al.* [2002], and *Kelemen et al.* [2003b]. The composition of altered basalt was taken from *Bach et al.* [2003]. All data and models are normalized by the primitive mantle composition of *McDonough and Sun* [1995]. Data for Batan inclusions and inclusion-rich olivines are taken from *Schiano et al.* [1995]. See the auxiliary material for the distribution coefficients and the altered basalt compositions used to calculate all model melt compositions.

ments [*Plank and Langmuir*, 1998]) in the metasomatic melts and/or fluids that infiltrated them.

[26] Trace element patterns of all seven model eclogite melts plotted in Figure 3b resemble those of Batan inclusions in several respects: they have similar overall enrichments of highly incompatible elements relative to moderately incompatible and compatible elements, and all share a positive anomaly in Sr and negative anomalies in Ba and Nb. These are among the reasons why previous study of Batan inclusions suggested they were well explained as slab melts [*Schiano et al.*, 1995].

[27] On the other hand, there are also several differences between these model slab melts and

Batan inclusions: Ba/Th ratios of Batan inclusions are ~2 to 5-times higher than predicted by any of these eclogite melting models; this could be explained by slab melting only if those slab sources were unusually Ba-rich. All models predict primitive-mantle-normalized U/Th ratios ("$(U/Th)_N$") lower than 1, whereas Batan inclusions have $(U/Th)_N$ ratios of ~1.5; thus slab-melting models of Batan inclusions would also require unusually U-rich sources. All slab-melting models that lack rutile in the residue yield U/Nb ratios lower by factors of ~5 to 20 than those observed in Batan inclusions. The models that contain 1% rutile in the residue can explain this feature. However, it is not clear whether Batan inclusions could be derived from rutile-bearing residues. Batan inclusions contain only 0.25 wt.% TiO_2, lower by a factor of 3.5 than the most TiO_2-poor rutile-saturated eclogite melts produced by eclogite melting experiments at shallow mantle pressures, and far lower than most such melts (typically 2–6 wt.% TiO_2 [*Rapp and Watson*, 1995; *Pertermann and Hirschmann*, 2003]). It is possible that some combination of previously unexplored temperatures, pressures, source compositions and degrees of melting will yield appropriately low-Ti melts of rutile-bearing eclogite sources. Also, one might imagine ways of lowering the Ti contents of slab melts by reaction with the mantle wedge [*Kelemen et al.*, 1990]. Nevertheless, the Ti contents of Batan inclusions are clearly lower than expected for melts of rutile-bearing eclogite based on published experimental constraints, and thus the high U/Nb ratios of these inclusions are poorly explained by slab melting.

[28] Batan inclusions are characterized by a large positive Pb anomaly. Neither of the two experimental studies of eclogite melting produced melts with this feature. The models that use estimated distribution coefficients based on data from non-eclogitic systems (models "Kelemen" and "Salters" in Figure 3b) produce Pb anomalies nearly as large as that in Batan inclusions, but the low solid/melt Pb distribution coefficients they require have not yet been confirmed by experiment. *Kamber et al.* [2002] present an analysis of Pb abundances in arc-related lavas that relates to this issue. Pb/Nd ratios (an approximate measure of the size of the Pb anomaly) in typical island arc basalts average 0.5, strongly elevated relative to values of primitive or depleted mantle (0.12 and 0.04, respectively) or altered MORB (0.09). *Kamber et al.* [2002] attribute this characteristic of arc lavas to preferential extraction of Pb from subducted slabs on release of aqueous fluid. Adakites typically have lower Pb/Nd ratios of approximately 0.35, more consistent with ratios expected for slab-derived melts [*Kamber et al.*, 2002]. Pb/Nd ratios of Batan inclusions average 1.9, greatly in excess of adakites or even normal arc basalts and, in the context of *Kamber et al.*'s [2002] interpretation, strongly indicative of enrichment in fluid-soluble elements relative to "normal" subducting crust.

[29] All model eclogite melts have negative Zr anomalies and positive Sr anomalies, resulting in $(Sr/Zr)_N$ ratios between ~5 and ~50. Measured $(Sr/Zr)_N$ ratios of Batan inclusions are only modestly elevated, averaging only 1.5, and these inclusions do not have negative Zr anomalies.

[30] Finally, experimental eclogite melts are characterized by pronounced depletions in heavy rare earths and Y due to compatibility of these elements in garnet, but relatively high contents of Ti. As a result, all four models based on distribution coefficients observed in eclogite melting experiments yield high $(Ti/Y)_N$ ratios (from ~20 for model "Xiong" to ~4.6 for model "Kessel"; Figure 3b). Lower ratios are predicted by the "Kelemen" models (2.1, or 1.8 with residual rutile) because this model assumes an exceptionally high solid/melt distribution coefficient for Ti in the silicate phases in eclogite. Nevertheless, even these ratios are far higher than those in Batan inclusions (average $(Ti/Y)_N$ ratio of ~0.7). Similarly, Batan inclusions are characterized by a negative Ti anomaly and none of the model melts have such a feature.

[31] Trace element partitioning during eclogite melting is relatively poorly understood, and it is possible that future work will reconcile the above-noted differences between Batan inclusions and model eclogite melts. Moreover, our model estimates are based on the altered ocean crust composition as given by *Bach et al.* [2003]. This estimate is based on a large body of evidence, but it is possible that some of the discrepancies we have noted could simply reflect an unexpected composition for the crust subducted beneath Batan. Nevertheless, these discrepancies pose a number of difficulties for slab melting models of the origin of Batan inclusions, and it is noteworthy that several of these discrepancies involve elements that are relatively soluble in aqueous fluids (Ba, U, Pb).

5.2. High-Pressure Differentiation of Island Arc Basalt?

[32] *Macpherson et al.* [2006] presented a model for the origins of adakites from Mindanau, the

Philippines, involving high-pressure (~1 Gpa; comparable to the depth from which Batan xenoliths come) differentiation of hydrous island arc basalt in the upper levels of the mantle wedge. At these pressures, precipitation of garnet and amphibole can yield residual liquids with characteristic adakitic trace element compositions (i.e., low abundances of Y and heavy rare earths and high Sr/Y ratios). Moreover, because many island arc basalts are derived from mantle sources that were metasomatized by slab-derived aqueous fluids prior to or during partial melting, this process could yield broadly adakitic liquids having positive anomalies in fluid-soluble trace elements and high ratios of relatively fluid-soluble to relatively fluid-insoluble elements (e.g., Pb/Ce, Ba/Th, U/Th and U/Nb), as we observe for Batan inclusions (Figure 3a). Finally, we estimate, on the basis of major element compositions of Batan island basalts [*Sajona et al.*, 2000], phase assemblages that crystallize from such basalts at high pressure [*Muntener et al.*, 2001], and oxygen isotope fractionations among relevant minerals and silicate melts [*Eiler*, 2001, and references therein], that the required tens of % crystallization should only lead to increases of ~0.2 to 0.5‰ in the $\delta^{18}O$ of the residual melt. Given that island arc basalts, even those with pronounced geochemical signatures of slab-derived components, generally have $\delta^{18}O$ values within ~0.5‰ of typical mantle-derived basalts [*Eiler et al.*, 2000], this process could generate liquids with $\delta^{18}O$ values near equilibrium with mantle peridotite, as we observe for Batan inclusions.

[33] *Macpherson et al.* [2006] present a model for high-pressure crystallization that can be compared with the trace element compositions of Batan inclusions and related lavas. Their description of high-pressure differentiation yields an expected trend of increasing Sr/Y ratio with decreasing Y content that has its sharpest increase toward relatively high Sr/Y (>50) at moderate Y concentration (~10 ppm; Figure 4a). The trend in Figure 4a defined by Batan basalts, basaltic andesites and the Batan inclusions examined in this study broadly resembles that predicted by the Macpherson et al. model, although Batan inclusions increase toward high Sr/Y at somewhat lower Y content (~5 ppm Y). We examine this model further in Figure 4b by comparing the Sr/Y ratio versus the MgO content for model hydrous basalt undergoing high-pressure crystallization with data for Batan inclusions and related lavas. High-pressure crystallization-differentiation is predicted to produce a nearly linear trend of monotonically increasing Sr/Y ratio with decreasing MgO content. In contrast, Batan lavas vary over a wide range in MgO (from ~10 to 2.5 wt.%) with no consistent trend in Sr/Y ratio, and Batan inclusions depart markedly from that trend toward high Sr/Y at ~1 wt.% MgO. The few Batan lavas that have Sr/Y ratios within the "adakitic" range (~50 or higher) are distributed seemingly randomly across the entire observed range in MgO. It is possible that the data trend for Batan lavas and inclusions plotted in Figure 4b reflects both high- and low-pressure differentiation in some combination that obscures the trend predicted by the model of *Macpherson et al.* [2006]. Nevertheless, there is no simple relationship between Sr/Y ratio and differentiation in the Batan suites, despite the fact that this suite defines simple, continuous geochemical trends in other dimensions (e.g., Figure 1). Thus, while it is possible that the adakitic trace element compositions of Batan inclusions are a result of high-pressure crystallization, there is no clear evidence that this is the case.

5.3. Low-Degree Melting of Metasomatized Mantle-Wedge Peridotite?

[34] In this section, we examine whether Batan inclusions can be explained as low-degree melts of metasomatized mantle wedge peridotite. This hypothesis is motivated by two factors: (1) the $\delta^{18}O$ values of Batan inclusions are indistinguishable from those expected of peridotite partial melts, and (2) their trace element compositions are characterized by several features that are expected for melts of sources metasomatized by slab-derived aqueous fluids, including high Ba/Th, U/Th, U/Nb, and Pb/Ce [*Brenan et al.*, 1995a, 1995b; *Keppler*, 1996; *Stalder et al.*, 1998; *Kessel et al.*, 2005b]. Similarly, although the partitioning behavior of Cu is not well-known, previous studies of island arc and back-arc lavas have found that pronounced enrichments in Cu, comparable to those seen in Batan inclusions, are associated with enrichments in other fluid-soluble elements [*Stolper and Newman*, 1994; *Eiler et al.*, 2005]. We are not aware of any previous discussion of Sn anomalies in arc-related magmas, but present these data for possible future reference.

[35] Partial melting experiments conducted on peridotites and synthetic peridotite analogues show that alkali-rich melts formed at pressures less than 1.5 GPa can have silica contents approaching those of Batan melt inclusions [*Hirschmann et al.*, 1998, and references therein]. In the absence of water and using natural starting materials, these experiments

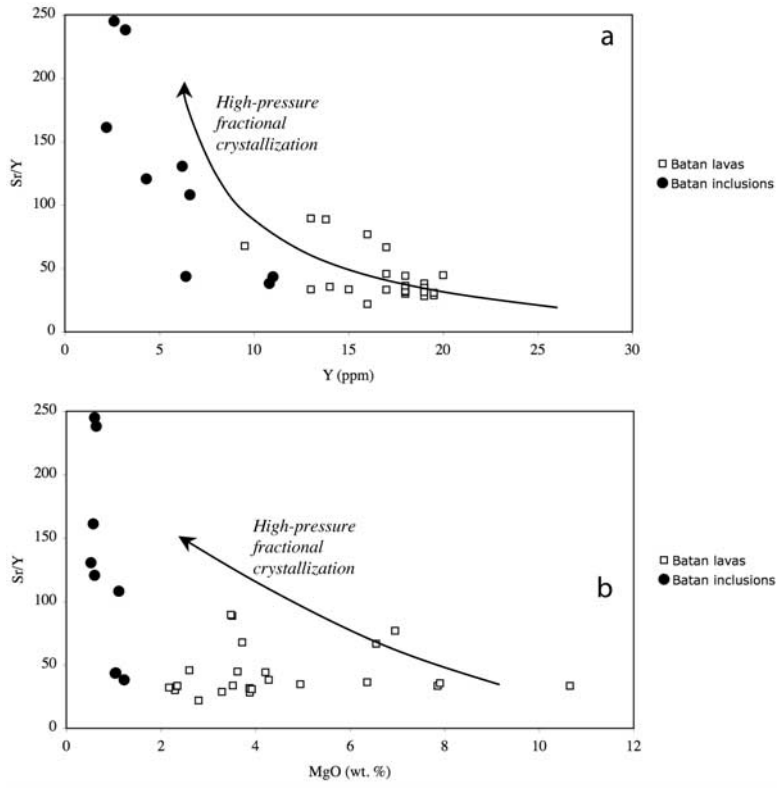

Figure 4. Comparison of trends in (a) Sr/Y versus Y and (b) Sr/Y versus MgO for Batan inclusions (filled circles; data from *Schiano et al.* [1995] and the auxiliary material of this paper) and related lavas (unfilled squares; data from *Sajona et al.* [2000]) with predicted trends for a model of high-pressure crystallization of hydrous basalt (solid curves). The model trend assumes a fractionating assemblage and trace element distribution coefficients as given by *Macpherson et al.* [2006], mineral compositions from experiment B726 of *Muntener et al.* [2001], an initial MgO content of 9 wt.%, and initial Sr and Y contents of 500 and 14 ppm, respectively, based on data for Batan island lavas from *Sajona et al.* [2000]. The model trends represent 0 to 50 wt.% crystallization, with arrows indicating the direction of increasing extent of crystallization. High-pressure differentiation predicts trends of Sr/Y versus Y that broadly resemble those of Batan inclusions and lavas, but does not resemble the distribution of data in dimensions of Sr/Y versus MgO.

fail to produce silica contents quite as high as those of Batan inclusions (avg. 59.6 wt.% SiO_2 [*Schiano et al.*, 1995]) at appropriate total alkali contents (7 to 8 wt.% $Na_2O + K_2O$). However, Batan glass inclusions contain ~5 wt.% H_2O (and likely contained even more before exsolving a water-rich fluid), so the combined influences of high alkali and water contents could be sufficient to produce such high silica contents in low-degree, low-pressure melts of peridotite [*Hirschmann et al.*, 1998, 1999; *Gaetani and Grove*, 1998, 2003]. 1.2 GPa experiments by *Draper and Green* [1999] have shown that liquids with ~60 wt.% SiO_2, ~13 wt.% $Na_2O + K_2O$ and ~2.5 wt.% $H_2O + CO_2$ are saturated with olivine, orthopyroxene and clinopyroxene at 1150°C. The MgO contents and Mg/Fe ratios of Batan inclusions are far lower than those of experimental peridotite melts, including Si- and H-rich melts. Given the evidence for formation of metasomatic hydrous phases and neoblastic olivine and orthopyroxene in Batan xenoliths, this could reflect modification of the major element compositions of Batan inclusions by crystallization-differentiation before, during and/or after inclusion entrapment. We conclude that the major element compositions of Batan inclusions are not clearly distinctive of peridotite melts, but could be peridotite melts that were modified by crystallization-differentiation.

[36] We further examine this hypothesis by way of the following trace element model: Batan xenoliths and abyssal peridotites from the Bouvet fracture zone [*Johnson et al.*, 1990] are similar to one another in their modal abundances of clinopyroxene [*Maury et al.*, 1992; *Johnson et al.*, 1990], and Bouvet peridotites appear to be typical examples of

the residues of high degrees of fractional melting. Consequentially, we describe a model peridotitic source for Batan inclusions, prior to being metasomatized, as a depleted peridotite having a trace element composition similar to harzburgites from the Bouvet fracture zone. *Johnson et al.* [1990] analyzed only select elements in clinopyroxene from the Bouvet fracture zone, so we extend their results to other elements of interest by assuming clinopyroxenes have smooth chondrite-normalized trace element patterns for elements as or more compatible than Nb (i.e., interpolating between *Johnson et al.*'s [1990] measurements of Ce, Nd, Zr, Sr, Sm, Ti and Yb), and contain no U, Th, Ba, Rb or Cs (i.e., budgets of these elements in our model metasomatized source are completely controlled by the metasomatic agent). We calculated the trace element contents of coexisting olivines, orthopyroxenes, and spinels by multiplying clinopyroxene compositions by the ratio of the relevant mineral-melt distribution coefficient to the clinopyroxene-melt distribution coefficient (using data from *Green and Pearson* [1983], *Colson et al.* [1988], *Kelemen et al.* [1990], *Hart and Dunn* [1993], *Kennedy et al.* [1993], *Nielsen et al.* [1993, 1994], and *Green* [1994]). The resulting model trace element composition of a depleted peridotite source closely resembles measured trace element compositions of whole-rock samples of harzburgites from the Voykar ophiolite [*Sharma et al.*, 1995]. We then added to this depleted peridotite 0.5 wt.% of a model metasomatic agent (i.e., so little that it will not substantially change the $\delta^{18}O$ of the metasomatized source even if that agent is slab-derived) and modeled 1% melting of the hybrid source (i.e., a low enough degree that product melt will contain tens of wt.% H_2O). We then solved for the composition of the metasomatic agent needed to produce a model melt having the composition of the average of Batan inclusions (i.e., by solving the set of simultaneous linear equations describing mineral-melt partitioning and mass balance, assuming the constraints described above; see Table S8 in the auxiliary material for relevant distribution coefficients).

[37] This calculation is representative of a family of broadly similar models that differ from one another in the degree of depletion of the mantle wedge prior to metasomatism, in the amount of metasomatic agent, and in the degree of melting of the hybrid source. Variations in these parameters lead to variations in absolute concentrations of trace elements in the model metasomatic agent required to fit the data for Batan inclusions. However, all successful models of this sort require initially depleted sources (i.e., prior to metasomatism), small amounts of slab-derived component, and enrichment in fluid-soluble elements in that slab-derived component. Table 2 presents the compositions of model depleted peridotite, the solved-for model metasomatic agent, and the model hybrid source.

[38] Figure 5a compares the model metasomatic fluid calculated using the above-described model to slab-derived components previously inferred to contribute to the sources of arc and back-arc lavas from a variety of geographic locations [*McCulloch and Gamble*, 1991; *Stolper and Newman*, 1994; *Eiler et al.*, 2000; *Grove et al.*, 2002] (and the "slab fluid" component from *Eiler et al.* [2005]). Our model metasomatic agent has relative abundances of Th, U, Nb, K, La and Ce that closely resemble those for all of these previously estimated slab-derived components (Figure 5a), but it has a significantly lower Ba/Th ratio. The Pb anomaly in our model metasomatic agent is similar in size to that for the slab-derived component of *McCulloch and Gamble* [1991], and greater than those for the slab-derived components of *Stolper and Newman* [1994] and *Grove et al.* [2002] (*Eiler et al.* [2000] did not estimate the Pb abundance in their slab-derived component). Middle-rare earth and Sr abundances in our model metasomatic agent resemble those for all of these previously estimated slab-derived components, although our model component has a smaller positive Sr anomaly and lacks the negative Zr anomaly shared by those components. It is possible that the difference in Zr content reflects our overestimation of the degree of prior depletion of the peridotite source of Batan inclusions prior to metasomatism. Such a change to our model of Batan inclusions would slightly lower all incompatible trace element concentrations in our model fluid and exaggerate its negative Nb and Ti anomalies. Finally, abundances of elements more compatible than Sm in our model metasomatic agent are at the low end of the range previously estimated for slab-derived components and most resemble those from *McCulloch and Gamble* [1991] and *Eiler et al.* [2005].

[39] Figure 5b compares the composition of our model metasomatic agent to compositions of various aqueous fluids and aqueous supercritical phases in equilibrium with altered oceanic crust [*Bach et al.*, 2003] in the eclogite facies, based on laboratory fluid/mineral or fluid/bulk eclogite partitioning experiments [*Brenan et al.*, 1995a, 1995b;

Table 2. Compositions of Model Components[a]

Element	Depleted Peridotite	Metasomatic Agent	Hybrid Source
Cs	0.0	12	0.06
Rb	0.0	250	1.25
Ba	0.0	1600	8.0
Th	0.0	26	0.13
U	0.0	10	0.05
Nb	0.000066	20	0.099
K	0.024	51500	258
La	0.000065	112	0.56
Ce	0.00043	192	0.96
Pb	0.000042	130	0.65
Pr	0.000081	27	0.14
Nd	0.00044	49	0.25
Zr	0.021	648	3.3
Sr	0.046	1570	7.9
Sm	0.0016	7.7	0.040
Eu	0.0011	1.1	0.0066
Gd	0.0054	6.5	0.038
Tb	0.0020	0.9	0.0065
Dy	0.020	3.0	0.035
Ti	43	2000	53
Y	0.13	10	0.18
Er	0.031	1.0	0.036
Yb	0.046	1.0	0.051
Cu	3.0	8000	43
Sn	0.00052	120	0.60

[a] All values are parts per million, by mass.

Stalder et al., 1998; *Kessel et al.*, 2005b]. Note that the model labeled "Kessel 6 GPa" uses data for partitioning between eclogite and a "melt-like" aqueous supercritical phase; this is the same as model "Kessel" in Figure 3b. We also show the expected composition of aqueous fluid in equilibrium with depleted mantle peridotite (*Ayers et al.* [1997] using the depleted mantle composition of *Workman and Hart* [2005]). In all cases, we assume equilibration between 1% fluid and 99% solid; a subset of these models assume 1% rutile in the solid, as indicated in the legend. We do not consider fluids in equilibrium with subducted marine sediment because, as mentioned above, metasomatized Batan xenoliths have $^{87}Sr/^{86}Sr$ ratios far too low for them to contain any appreciable amount of Sr from subducted sediment.

[40] The expected trace element concentrations in aqueous phases in equilibrium with subducted crust vary widely both in absolute concentrations (by two to three orders of magnitude for many elements) and in abundance ratios (e.g., U/Nb ratios of fluids in equilibrium with rutile-free eclogite differ by a factor of 20 between *Brenan et al.* [1995a, 1995b] and the 4 GPa experiment of *Kessel et al.* [2005b]). This diversity could reflect any of a number of differences between these various experiments, such as temperature, pressure, solution chemistry (e.g., chloride content), the presence or absence of rare but trace element-rich phases, and/or experimental artifacts such as partial equilibration or elemental gain to or loss from the experimental charge. One factor that clearly appears to be important is that concentrations of most elements increase, and positive and negative anomalies diminish, with increasing pressure. These changes occur over a relatively narrow range of pressure, from "fluid-like" low concentrations and large element-specific anomalies at 4 GPa to "melt-like" high concentrations and modest anomalies at 6 Gpa [*Kessel et al.*, 2005b].

[41] Our model metasomatic agent (filled circles in Figure 5b) is characterized by abundances of rare earth elements, Zr, Sr, and Nb that approach those for the 6 GPa supercritical aqueous phase in equilibrium with rutile-absent altered oceanic crust based on the results of *Kessel et al.* [2005b] (unfilled circles). On the other hand, the positive Pb anomaly, high U/Nb and U/Th ratios and high Cs, Rb and Ba contents relative to other incompatible elements characteristic of our model metasomatic agent more closely resemble aqueous fluid in equilibrium with subducted crust at somewhat lower pressures of 4 or 5 GPa [*Stalder et al.*, 1998; *Kessel et al.*, 2005b]. This apparent contradiction could indicate that our model metasomatic agent last equilibrated with a subducted slab at pressures between 4 and 6 GPa (and possibly at temperatures different from those examined by *Kessel et al.* [2005b]), and thus had a trace element composition intermediate to our "Kessel 4 GPa" and "Kessel-6 GPa" models. It is also possible that the sources of Batan inclusions were metasomatized by two or more components, one extracted from the slab at relatively high pressure and one at relatively low pressure, and our model metasomatic agent has averaged the compositions of these components.

[42] Despite the difficulty in matching our model metasomatic agent with a specific previous fluid-solid partitioning experiment, the generally "fluid-like" character of its trace element composition is confirmed by its Pb/Sr ratio. We are not aware that this ratio has been examined for such a purpose before, but it is useful because it involves two elements that are similarly incompatible during melting for all common silicate and oxide minerals at mantle pressures (i.e., excluding plagioclase), but strongly fractionated from one another during fluid/mineral partitioning. In this respect, it differs

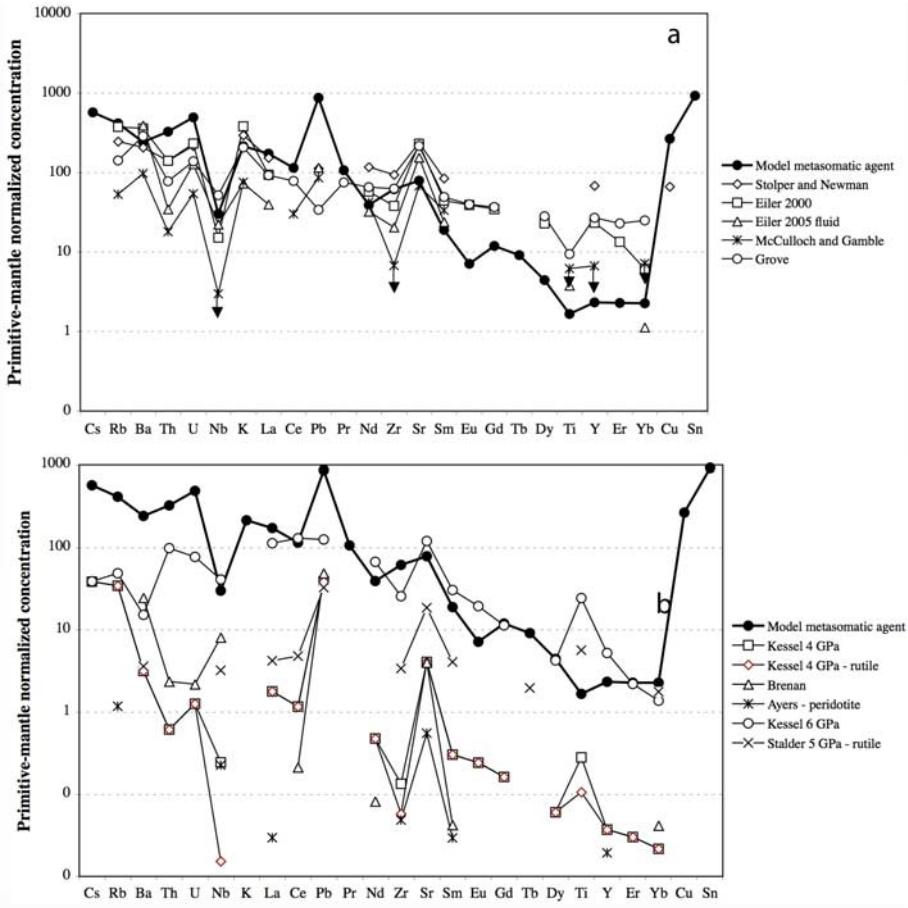

Figure 5. Comparison of the trace element composition of the calculated model metasomatic agent (Table 2) required to explain the compositions of Batan melt inclusions, assuming they formed by low degrees of melting of metasomatized depleted peridotite (see text), with (a) model slab-derived components previously inferred to contribute to the sources of arc lavas [*McCulloch and Gamble*, 1991; *Stolper and Newman*, 1994; *Eiler*, 2001; *Grove et al.*, 2002] (the ''aqueous fluid'' component of *Eiler et al.* [2005]) and (b) aqueous fluids or melts calculated to be in equilibrium with altered oceanic crust (based on partitioning experiments of *Brenan et al.* [1995a, 1995b] at 2 GPa; *Stalder et al.* [1998] at 5 GPa; and *Kessel et al.* [2005b] at 4–6 GPa) or with depleted mantle peridotite (based on partitioning experiments of *Ayers et al.* [1997]). Note that the data based on 6 GPa data from *Kessel et al.* [2005b] involve a broadly ''melt-like'' aqueous supercritical phase and were also included in Figure 3b. All models assume 1% fluid and 99% solid. Eclogites are assumed to be 60% garnet and 40% clinopyroxene (''Kessel 4 GPa –rutile'' and ''Stalder 5 GPa – rutile'' include 1% rutile) and to have the composition of altered basalt from *Bach et al.* [2003]. All models are normalized by the primitive mantle composition of *McDonough and Sun* [1995]. The depleted mantle model (''Ayers-peridotite'') assumes the solid is a peridotite having the composition of depleted mantle from *Workman and Hart* [2005] (interpolated to yield concentrations of Cs, K, and Pb). Distribution coefficients and source concentrations used to construct these models are provided in the auxiliary material.

from the U/Nb ratio, which can be elevated due to fluid/mineral partitioning or melting in the presence of residual rutile, and from the Sr/Sm and Pb/Ce ratios, which can be elevated by both fluid/mineral partitioning and by melting in the presence of residual garnet.

[43] Figure 6 compares the primitive-mantle-normalized Pb/Sr ratio of our model metasomatic agent and average Batan inclusions (horizontal bars) with the ratios expected of aqueous fluid, melt and aqueous supercritical phase in equilibrium with altered ocean crust. For comparison, we also show Pb/Sr ratios expected for melts of peridotitic depleted mantle. In each case, the modeled Pb/Sr ratios are plotted versus the fraction of fluid or melt, indicating the range of possible compositions that might result from variations in degree of dehydration or melting. Pb/Sr ratios of relatively low-pressure aqueous fluids (i.e., 2 GPa from *Brenan et al.* [1995a, 1995b] and 4 GPa from

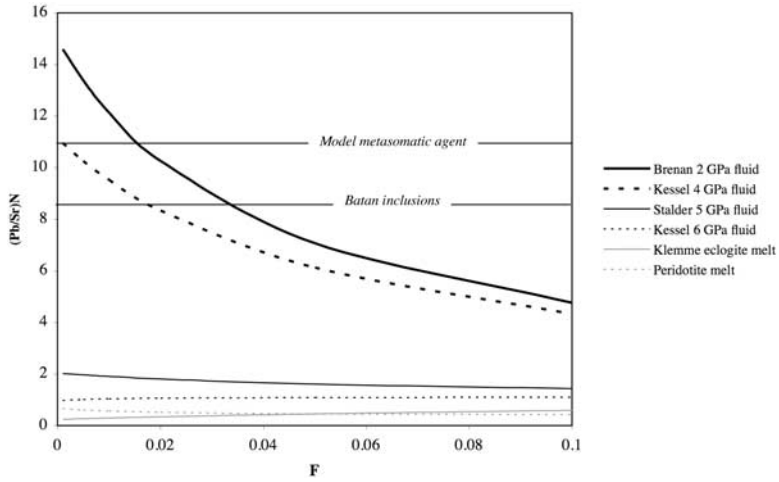

Figure 6. Comparison of the primitive-mantle-normalized Pb/Sr ratios ("$(Pb/Sr)_N$") of Batan inclusions and model metasomatic agent (horizontal lines) with $(Pb/Sr)_N$ ratios predicted for aqueous fluids in equilibrium with altered basalt (based on experiments of *Brenan et al.* [1995a, 1995b], *Stalder et al.* [1998], and *Kessel et al.* [2005b]), partial melt of altered basalt in the eclogite facies (based on data from *Klemme et al.* [2002]), and partial melt of depleted mantle peridotite (using distribution coefficients summarized by *Eiler et al.* [2005]). All models are plotted as functions of the fraction of melt or fluid (F). Distribution coefficients and source compositions used to construct these models are provided in the auxiliary material.

Kessel et al. [1995b, 2005b]) are an order of magnitude higher than those of any melt or aqueous supercritical phase at any degree of melting or dehydration; only 5 GPa aqueous fluid lies between these extremes. Our model metasomatic agent has a Pb/Sr ratio consistent only with those of relatively low-pressure ($\leq$4 GPa) slab-derived aqueous fluids. It is possible that this comparison is compromised by some artifact in the measurement of Pb/Sr ratios in Batan inclusions (e.g., selective enrichment in sulfide; although we consider this unlikely given the relative homogeneity in the size of the Pb anomaly exhibited by those measurements). It is also possible that the high Pb/Sr ratios seen in 2–4 GPa fluids are an experimental artifact caused by Pb loss from the experimental charge (although it is not obvious why this artifact would effect only the low-pressure fluid experiments). Despite these ambiguities, we suggest that the high Pb/Sr ratios of Batan inclusions strengthen the argument that fluid/mineral partitioning played an important role in their origin.

[44] More generally, Figure 6 provides insight into the possible roles of slab melts, fluids and aqueous supercritical phases in arc magma genesis. The primitive-mantle-normalized Pb/Sr ratios of island arc basalts generally vary between 1 and 1.5 [*McCulloch and Gamble*, 1991] and slab-derived components previously inferred to contribute to arc-related lavas are similarly low (e.g., 1.27 for *McCulloch and Gamble* [1991], 0.48 for *Stolper and Newman* [1994], 0.16 for *Grove et al.* [2002], and 0.75 for *Eiler et al.* [2005]). Thus arc-related magmas generally have Pb/Sr ratios far lower than those of low-pressure aqueous fluids in equilibrium with subducted slabs, and are better explained by slab contributions from slab-derived melt or aqueous supercritical phase. Batan inclusions (and the model metasomatic agent we infer controlled their trace element compositions), despite having many properties resembling slab-derived components elsewhere (Figure 5a), are clearly unusual in Pb/Sr ratio. One interpretation of this result is that a relatively low-pressure slab-derived aqueous fluid controls the compositions of Batan inclusions, but that such fluids are relatively minor contributors to the sources of most arc lavas (i.e., as compared to slab-derived melts or aqueous supercritical phases).

[45] Finally, we note that no experimentally based fluid compositions contain the negative Ti anomaly characteristic of our model metasomatic agent (as was also true for slab-derived melts; Figure 3b). Residual rutile can retain Ti in subducted slabs. We found this was not an acceptable explanation of the Ti contents of Batan inclusions if they are slab melts because rutile-saturated melts at relevant temperatures and pressures are too rich in TiO_2 [*Rapp and Watson*, 1995; *Pertermann and Hirschmann*, 2003]. However, it is possible that rutile-saturated aqueous fluids could have negative Ti anomalies under some conditions relevant to subducted slabs. This is an attractive target for further experimental

study. Reaction between melt and mantle-wedge peridotite can generate small negative Ti anomalies in melt [*Kelemen et al.*, 1990], but not sufficient to yield the low Ti/Y and low ratios of Ti to heavy rare earth elements ratios characteristic of Batan inclusions [*Rapp et al.*, 1999].

5.4. Implications for the Origins of Silica-Rich Convergent-Margin Magmas

[46] Batan inclusions fit the formal and common-usage definitions of adakites: i.e., they are silica-rich melts formed in a convergent margin and having Y contents less than ~20 ppm and Sr/Y ratios greater than ~50 [*Defant and Drummond*, 1990]. Therefore interpretations regarding the origins of Batan inclusions have relevance for the understanding of adakites (as well as compositionally similar adakite-like andesites). These lavas are widely believed to be slab-derived melts or products of reaction between slab-derived melts and peridotitic mantle wedge. This hypothesis has been challenged previously on the grounds that adakite-like melts can be generated through various mechanisms of basalt differentiation in the crust and upper mantle [*Atherton and Petford*, 1993; *Castillo et al.*, 1999; *Conrey et al.*, 2001; *Garrison and Davidson*, 2003; *Hou et al.*, 2004; *Wang et al.*, 2005; *Macpherson et al.*, 2006]. Our findings suggest that it is also possible to produce broadly adakitic melts by low-degree partial melting of metasomatized peridotite.

[47] Because diverse petrogenetic processes appear capable of generating broadly similar Sr/Y ratios and Y and SiO_2 contents (the variables most often used to define adakites), these indices cannot definitively distinguish slab-derived melts from basalt differentiates or melts of metasomatized mantle wedge. Furthermore, the $\delta^{18}O$ value we find for siliceous Batan inclusions is indistinguishable from values previously found for most adakites [*Bindeman et al.*, 2005] and this similarity strengthens the case that petrogenetic processes responsible for creating Batan inclusions could also be responsible for making other adakitic lavas. On the other hand, Batan inclusions differ in some respects from the most restrictive definitions of adakites. For example, *Martin et al.* [2005] suggest that true adakites are characterized by K_2O/Na_2O ratios of $\leq$0.42, whereas Batan inclusions are more potassic (K_2O/Na_2O = 0.5 to 1.0). Moreover, Batan inclusions have unusually high Pb/Sr ratios, which could be a signature of the relatively low-pressure fluid-solid trace element fractionations, and, similarly, are far higher in Pb/Nd than common adakites [*Kamber et al.*, 2002]. Thus it is possible that a sufficiently strict and detailed definition of adakites might discriminate silica-rich, peridotite-derived melts from slab-derived melts having broadly similar compositions.

[48] Batan inclusions define an end-member in the compositional trends defined by basalts and basaltic andesites from the Luzon arc (Figure 1). Therefore it seems reasonable to infer either that the Luzon magmas represent mixtures, and the inclusions represent one of the mixing components of those magmas, or that the inclusions reflect extreme instances of the same petrogenetic process that produced the erupted magmas. For example, it is possible that the mantle wedge beneath the Luzon arc is variably modified by the metasomatic agent we have modeled and melts to variable degree; in this case, the silica-rich inclusions reflect low-degree melts of these hybrid sources and lavas are derived from higher degree melts of the same or related sources.

[49] It is tempting to generalize further that the siliceous compositions and distinctive trace element compositions of arc lavas from places other than Batan could derive, at least in part, from the high silica contents of low-degree melts of hydrous, metasomatized peridotites. Indeed, the similarity of our model metasomatic agent to slab-derived components inferred in other subduction zones (Figure 5a) suggests that the petrogenetic process we describe for Batan inclusions could be an extreme manifestation of processes that generate more common convergent-margin basalts and andesites. However, it is not clear whether low-degree (~1% or less) melts can be extracted from mantle peridotites efficiently enough to create magma bodies sufficiently large to erupt lavas. Furthermore, some trace element characteristics of Batan inclusions (e.g., their high Pb/Sr ratios; Figure 6) are unusual and may indicate that the process that generates them rarely, if ever, controls the trace element budgets of erupted lavas.

6. Summary

[50] Silica-rich melt inclusions in peridotite xenoliths from Batan island (Luzon arc) are characterized by oxygen isotope compositions in equilibrium with average mantle peridotite. This result is inconsistent with the hypothesis that these inclusions are direct partial melts of weathered or altered components of the subducted slab beneath the Luzon arc, which

generally differ in $\delta^{18}O$ from common mantle peridotites. The Sr isotope compositions of inclusion-rich xenoliths also cannot be easily reconciled with inclusions being direct melts of subducted sediment. Moreover, the trace element compositions of Batan inclusions contrast in several respects with those expected for melts of basalt in the eclogite facies, so our results are not well explained by way of some process that selectively influenced oxygen isotope compositions of slab melts (such as isotopic exchange of compatible elements like oxygen during transport through the mantle wedge). Batan inclusions and related lavas lack the correlated changes in Sr/Y and MgO expected to result from high-pressure crystallization of island arc basalts (Figure 4b); thus, if they are products of differentiation, it must have occurred at low pressure, or over a range of conditions that obscures the predicted high-pressure trend.

[51] The oxygen isotope compositions of Batan inclusions can be explained if they are partial melts of peridotites from the mantle wedge. The major and trace element compositions of these inclusions can also be explained by such a process, provided their peridotite source was metasomatized by a slab-derived, water-rich phase before or during partial melting, and that the low MgO contents and Mg/Fe ratios of Batan inclusions can be attributed to crystallization-differentiation before, during or after inclusion entrapment. We estimate the composition of the metasomatic agent required to explain the compositions of Batan inclusions using a partial melting model similar to those previously used to explain the trace element compositions of arc lavas. We find that the properties of this model metasomatic phase are broadly consistent with an aqueous fluid that equilibrated with altered basalt at pressures of ~4–6 GPa (only the TiO_2 content of Batan inclusions is not well explained by this process). Our model metasomatic agent resembles slab-derived components previously inferred to contribute to the sources of arc-related basalts and andesites, suggesting that the processes responsible for generating Batan inclusions could be related to the petrogenesis of more common arc lavas.

[52] Melt inclusions from Batan xenoliths have been previously interpreted as slab melts, and their compositional similarity to adakites has been regarded as evidence that adakites are also slab-derived melts. Our finding that Batan inclusions could be partial melts of metasomatized mantle peridotites suggests an alternative interpretation of adakites; i.e., that some could be produced by metasomatism of peridotitic mantle wedge by hydrous slab-derived components, followed by partial melting of the hybrid source.

Acknowledgments

[53] We thank Rene Maury for providing access to the sample examined in this study and for his help and guidance during the early stages of this work. This study benefited from financial support from NSF grant EAR-0337736 and a grant to J.M.E. from the Packard foundation. This work benefited from reviews by P. Kelemen, C. Macpherson, J. Ryan, and G. Gaetani. We thank G. Bebout and V. Salters for their work editing this paper.

References

Alt, J. C., K. Muehlenbachs, and J. Honnorez (1986), An oxygen isotopic profile through the upper kilometer of the oceanic crust, DSDP hole 504B, *Earth Planet. Sci. Lett.*, *80*, 217–229.

Arthur, M. A., T. F. Anderson, and I. R. Kaplan (1983), *Stable Isotopes in Sedimentary Geology, SEPM Short Course*, *10*, 432 pp.

Atherton, M. P., and N. Petford (1993), Generation of sodium-rich magmas from newly underplated basaltic crust, *Nature*, *362*, 144–146.

Ayers, J. C., S. K. Dittmer, and G. D. Layne (1997), Partitioning of elements between peridotite and H_2O at 2.0–3.0 GPa and 900–1100 degrees C, and application to models of subduction zone processes, *Earth Planet. Sci. Lett.*, *150*, 381–398.

Bach, W., B. Peucker-Ehrenbrink, S. R. Hart, and J. S. Blusztajn (2003), Geochemistry of hydrothermally altered oceanic crust: DSDP/ODP Hole 504B – Implications for seawater-crust exchange budgets and Sr- and Pb-isotopic evolution of the mantle, *Geochem. Geophys. Geosyst.*, *4*(3), 8904, doi:10.1029/2002GC000419.

Baker, L. J., P. M. Smith, P. D. Asimow, C. E. Hall, and M. C. Gurnis (2005), GyPSM-S: A synthesis model for fully-coupled geodynamic and petrological flow calculations related to subduction, *Eos Trans. AGU*, *86*(52), Fall Meet, Suppl., Abstract T31D-01.

Baker, M. B., M. M. Hirschmann, M. S. Ghiorso, and E. M. Stolper (1995), Compositions of near-solidus peridotite melts from experiments and thermodynamic calculations, *Nature*, *375*, 308–311.

Billen, M. I., and M. Gurnis (2001), A low viscosity wedge in subduction zones, *Earth Planet. Sci. Lett.*, *193*, 227–236.

Bindeman, I. N., J. M. Eiler, G. M. Yogodzinski, Y. Tatsumi, C. R. Stern, T. L. Grove, M. Portnyagin, K. Hoernle, and L. V. Danyushevsky (2005), Oxygen isotope evidence for slab melting in modem and ancient subduction zones, *Earth Planet. Sci. Lett.*, *235*, 480–496.

Brenan, J. M., H. F. Shaw, and F. J. Ryerson (1995a), Experimental evidence for the origin of lead enrichment in convergent-margin magmas, *Nature*, *378*, 54–56.

Brenan, J. M., H. F. Shaw, F. J. Ryerson, and D. L. Phinney (1995b), Mineral-aqueous fluid partitioning of trace elements at 900°C and 2.0 GPa: Constraints on the trace element geochemistry of mantle and deep crustal fluids, *Geochim. Cosmochim. Acta*, *59*, 3331–3350.

Castillo, P. R., P. E. Janney, and R. U. Solidum (1999), Petrology and geochemistry of Camiguin Island, southern Philippines:

Insights to the source of adakites and other lavas in a complex arc setting, *Contrib. Mineral. Petrol.*, *134*, 33–51.

Chung, S. L., D. Y. Liu, J. Q. Ji, M. F. Chu, H. Y. Lee, D. J. Wen, C. H. Lo, T. Y. Lee, Q. Qian, and Q. Zhang (2003), Adakites from continental collision zones: Melting of thickened lower crust beneath southern Tibet, *Geology*, *31*, 1021–1024.

Colson, R. O., G. A. McKay, and L. A. Taylor (1988), Temperature and composition dependencies of trace element partitioning; olivine/melt and low-Ca pyroxene melt, *Geochim. Cosmochim. Acta*, *52*, 539–553.

Condie, K. C., and D. H. Swenson (1973), Compositional variations in three Cascade stratovolcanoes: Jefferson, Rainier and Shasta, *Bull. Volcanol.*, *37*, 205–320.

Conrey, R. M., P. R. Hooper, P. B. Larson, J. Chesley, and J. Ruiz (2001), Trace element and isotopic evidence for two types of crustal melting beneath a High Cascade volcanic center, Mt. Jefferson, Oregon, *Contrib. Mineral. Petrol.*, *141*, 710–732.

Davidson, J. P. (1996), Deciphering mantle and crustal signatures in subduction zone magmatism, in *Subduction: Top to Bottom*, *Geophys. Monogr. Ser.*, vol. 96, edited by G. E. Bebout et al., pp. 251–262, AGU, Washington, D. C.

Davies, J. H., and M. J. Bickle (1991), A physical model for the volume and composition of melt produced by hydrous fluxing above subduction zones, *Philos. Trans. R. Soc. London, Ser. A*, *33*, 355–364.

Davies, J. H., and D. J. Stevenson (1992), Physical model of source region of subduction zone volcanics, *J. Geophys. Res.*, *97*, 2037–2070.

Defant, M. J., and M. S. Drummond (1990), Derivation of some modern arc magmas by melting of young subducted lithosphere, *Nature*, *347*, 662–665.

Draper, D. S., and T. H. Green (1999), P-T phase relations of silicic, alkaline, aluminous liquids: New results and applications to mantle melting and metasomatism, *Earth Planet. Sci. Lett.*, *170*, 255–268.

Ducea, M., G. Sen, J. Eiler, and J. Fimbres (2002), Melt depletion and subsequent metasomatism in the shallow mantle beneath Koolau volcano, Oahu (Hawaii), *Geochem. Geophys. Geosyst.*, *3*(2), 1015, doi:10.1029/2001GC000184.

Eiler, J. M. (2001), Oxygen isotope variations of basaltic lavas and upper mantle rocks, in *Stable Isotope Geochemistry*, *Rev. Mineral. Geochem.*, vol. 43, edited by J. W. Valley and D. R. Cole, pp. 319–364, Mineral. Soc. of Am., Washington, D. C.

Eiler, J. M., K. A. Farley, J. W. Valley, E. Hauri, H. Craig, S. Hart, and E. M. Stolper (1996), Oxygen isotope variations in ocean island basalt phenocrysts, *Geochim. Cosmochim. Acta*, *61*, 2281–2293.

Eiler, J. M., C. Graham, and J. W. Valley (1997), SIMS analysis of oxygen isotopes: Matrix effects in complex minerals and glasses, *Chem. Geol.*, *138*, 221–244.

Eiler, J. M., B. McInnes, J. W. Valley, C. M. Graham, and E. M. Stolper (1998), Oxygen isotope evidence for slab-derived fluids in the sub-arc mantle, *Nature*, *393*, 777–781.

Eiler, J. M., A. Crawford, T. Elliott, K. A. Farley, J. W. Valley, and E. M. Stolper (2000), Oxygen isotope geochemistry of oceanic-arc lavas, *J. Petrol.*, *41*, 229–256.

Eiler, J. M., M. J. Carr, M. Reagan, and E. Stolper (2005), Oxygen isotope constraints on the sources of Central American arc lavas, *Geochem. Geophys. Geosyst.*, *6*, Q07007, doi:10.1029/2004GC000804.

Elliott, T., T. Plank, A. Zindler, W. White, and B. Bourdon (1997), Element transport from slab to volcanic front at the Mariana arc, *J. Geophys. Res.*, *102*, 14,991–15,019.

Gaetani, G. A., and T. L. Grove (1998), Influence of water on melting of mantle peridotite, *Contrib. Mineral. Petrol.*, *131*, 323–346.

Gaetani, G. A., and T. L. Grove (2003), Experimental constraints on melt generation in the mantle wedge, in *Inside the Subduction Factory*, *Geophys. Monogr. Ser.*, vol. 138, edited by J. Eiler, pp. 107–134, AGU, Washington D. C.

Garrison, J. M., and J. P. Davidson (2003), Dubious case for slab melting in the northern volcanic zone of the Andes, *Geology*, *31*, 565–568.

Gill, J. B. (1981), *Orogenic Andesites and Plate Tectonics*, 390 pp., Springer, Berlin.

Green, D. H., and A. E. Ringwood (1967), The genesis of basaltic magmas, *Contrib. Mineral. Petrol.*, *5*, 103–190.

Green, T. H. (1994), Experimental studies of trace-element partitioning applicable to igneous petrogenesis—Sedona 16 years later, *Chem. Geol.*, *117*, 1–36.

Green, T. H., and N. J. Pearson (1983), Effect of pressure on rare-earth element partition coefficients in common magmas, *Nature*, *305*, 414–416.

Gregory, R. T., and H. P. Taylor (1981), An oxygen isotope profile in a section of the Cretaceous oceanic crust, Samail ophiolite, Oman: Evidence for $\delta^{18}O$ buffering of the oceans by deep (>5 km) seawater-hydrothermal circulation at mid-ocean ridges, *J. Geophys. Res.*, *86*, 2737–2755.

Grove, T. L., S. W. Parman, S. A. Bowring, R. C. Price, and M. B. Baker (2002), The role of an H_2O-rich fluid component in the generation of primitive basaltic andesites and andesites from the Mt. Shasta region, N. California, *Contrib. Mineral. Petrol.*, *142*, 375–396.

Hart, S. R., and T. Dunn (1993), Experimental cpx/melt partitioning of 24 trace elements, *Contrib. Mineral. Petrol.*, *113*, 1–8.

Hirschmann, M. M., M. B. Baker, and E. M. Stolper (1998), The effect of alkalis on the silica content of mantle-derived melts, *Geochim. Cosmochim. Acta*, *62*, 883–902.

Hirschmann, M. M., P. D. Asimow, M. S. Ghiorso, and E. M. Stolper (1999), Calculation of peridotite partial melting from thermodynamic models of minerals and melts. III. Controls on isobaric melt production and the effect of water on melt production, *J. Petrol.*, *40*, 831–851.

Hirth, G., and D. Kohlstedt (2003), Rheology of the upper mantle and the mantle wedge: A view from the experimentalists, in *Inside the Subduction Factory*, *Geophys. Monogr. Ser.*, vol. 138, edited by J. Eiler, pp. 83–106, AGU, Washington D. C.

Hou, Z. Q., Y. F. Gao, X. M. Qu, Z. Y. Rui, and X. X. Mo (2004), Origin of adakitic intrusives generated during mid-Miocene east-west extension in southern Tibet, *Earth Planet. Sci. Lett.*, *220*, 139–155.

Johnson, K. T. M., H. J. B. Dick, and N. Shimizu (1990), Melting in the oceanic upper mantle: An ion microprobe study of diopsides in abyssal peridotites, *J. Geophys. Res.*, *95*, 2661–2678.

Kamber, B. S., A. Ewart, K. D. Collerson, M. C. Bruce, and G. D. McDonald (2002), Fluid-mobile trace element constraints on the role of slab melting and implications for Archaean crustal growth models, *Contrib. Mineral. Petrol.*, *144*, 38–56.

Kay, R. W. (1978), Aleutian magnesian andesites: Melts from subducted Pacific Ocean crust, *J. Volcanol. Geotherm. Res.*, *4*, 117–132.

Kelemen, P. B. (1990), Reaction between ultramafic rock and fractionating basaltic magma. 1. Phase-relations, the origin of calc-alkaline magma series, and the formation of discordant dunite, *J. Petrol.*, *31*, 51–98.

Kelemen, P. B. (1995), Genesis of high Mg# andesites and the continental crust, *Contrib. Mineral. Petrol.*, *120*, 1–19.

Kelemen, P. B., K. T.M. Johnson, R. J. Kinzler, and A. J. Irving (1990), High field strength element depletions in arc basalts due to mantle-magma interactions, *Nature*, *345*, 521–524.

Kelemen, P. B., J. L. Rilling, E. M. Parmentier, L. Mehlm, and B. R. Hacker (2003a), Thermal structure due to solid-state flow in the mantle wedge beneath arcs, in *Inside the Subduction Factory*, *Geophys. Monogr. Ser.*, vol. 138, edited by J. Eiler, pp. 293–311, AGU, Washington D. C.

Kelemen, P. B., G. M. Yogodzinski, and D. W. Scholl (2003b), Along-strike variation in lavas of the Aleutian island arc: Genesis of high Mg# andesites and implications for continental crust, in *Inside the Subduction Factory*, *Geophys. Monogr. Ser.*, vol. 138, edited by J. Eiler, pp. 223–276, AGU, Washington D. C.

Kelley, K. A., T. Plank, L. Farr, J. Ludden, and H. Staudigel (2005), Subduction cycling of U, Th, and Pb, *Earth Planet. Sci. Lett.*, *234*, 369–383.

Kennedy, A. K., G. E. Lofgren, and G. J. Wasserburg (1993), An experimental study of trace element partitioning between olivine, orthopyroxene and melt in chondrules: Equilibrium values and kinetic effects, *Earth Planet. Sci. Lett.*, *115*, 177–195.

Keppler, H. (1996), Constraints from partitioning experiments on the composition of subduction-zone fluids, *Nature*, *380*, 237–240.

Kessel, R., P. Ulmer, T. Pettke, M. W. Schmidt, and A. B. Thompson (2005a), The water-basalt system at 4 to 6 GPa: Phase relations and second critical endpoint in a K-free eclogite at 700 to 1400 degrees C, *Earth Planet. Sci. Lett.*, *237*, 873–892.

Kessel, R., M. W. Schmidt, P. Ulmer, and T. Pettke (2005b), Trace element signature of subduction-zone fluids, melts and supercritical liquids at 120–180 km depth, *Nature*, *437*, 724–727.

Kita, N. T., Y. Ikeda, S. Togashi, Y. Z. Liu, Y. Morishita, and M. K. Weisberg (2004), Origin of ureilites inferred from a SIMS oxygen isotopic and trace element study of clasts in the Dar al Gani 319 polymict ureilite, *Geochim. Cosmochim. Acta*, *68*(20), 4213–4235.

Klemme, S., J. D. Blundy, and B. J. Wood (2002), Experimental constraints on major and trace element partitioning during partial melting of eclogite, *Geochim. Cosmochim. Acta*, *66*, 3109–3123.

Kolodny, Y., and S. Epstein (1976), Stable isotope geochemistry of deep sea cherts, *Geochim. Cosmochim. Acta*, *40*, 1195–1209.

Kushiro, I., Y. Syono, and S. Akimoto (1968), Melting of a peridotite nodule at high pressures and high water pressures, *J. Geophys. Res.*, *73*, 6023–6029.

Macpherson, C. G., S. T. Dreher, and M. F. Thirlwall (2006), Adakites without slab melting: High pressure differentiation of island arc magma, Mindanao, the Philippines, *Earth Planet. Sci. Lett.*, *243*, 581–593.

Martin, H. (1986), Effect of steeper Archean geothermal gradient on geochemistry of subduction-zone magmas, *Geology*, *14*, 753–756.

Martin, H. (1988), Archaean and modern granitoids as indicators of changes in geodynamic processes, *Rev. Bras. Geosci.*, *17*, 360–365.

Martin, H., R. H. Smithies, R. Rapp, J. F. Moyen, and D. Champion (2005), An overview of adakite, tonalite-trondhjemite-granodiorite (TTG), and sanukitoid: Relationships and some implications for crustal evolution, *Lithos*, *79*, 1–24.

Mattey, D., D. Lowry, and C. Macpherson (1994), Oxygen isotope composition of mantle peridotite, *Earth Planet. Sci. Lett.*, *128*, 231–241.

Maury, R. C., M. J. Defant, and J. L. Joron (1992), Metasomatism of the sub-arc mantle inferred from trace elements in Philippine xenoliths, *Nature*, *360*, 661–663.

McCulloch, M. T., and J. A. Gamble (1991), Geochemical and geodynamical constraints on subduction zone magmatism, *Earth Planet. Sci. Lett.*, *102*, 358–374.

McDermott, F., M. J. Defant, C. J. Hawkesworth, R. C. Maury, and J. L. Joron (1993), Isotope and trace-element evidence for 3 component mixing in the genesis of the north Luzon arc lavas (Philippines), *Contrib. Mineral. Petrol.*, *113*, 9–23.

McDonough, W. F., and S. S. Sun (1995), The composition of the Earth, *Chem. Geol.*, *120*, 223–253.

Muntener, O., P. B. Kelemen, and T. L. Grove (2001), The role of H_2O during crystallization of primitive arc magmas under uppermost mantle conditions and genesis of igneous pyroxenites: An experimental study, *Contrib. Mineral. Petrol.*, *141*, 643–658.

Nielsen, R. L., L. R. Forsythe, and M. R. Fisk (1993), The partitioning of HFSE between magnetite and natural mafic to intermediate liquids at low pressure, *Eos Trans. AGU*, *74*, 338–339.

Nielsen, R. L., W. E. Gallahan, and F. Newberger (1994), Experimentally determined mineral-melt partition coefficients for Sc, Y and REE for olivine, orthopyroxene, pigeonite, magnetite and ilmenite, *Contrib. Mineral. Petrol.*, *110*, 488–499.

O'Nions, R. K., and D. McKenzie (1988), Melting and continent generation, *Earth Planet. Sci. Lett.*, *90*, 449–456.

Peacock, S. M. (2003), Thermal structure and metamorphic evolution of subducting slabs, in *Inside the Subduction Factory*, *Geophys. Monogr. Ser.*, vol. 138, edited by J. Eiler, pp. 7–22, AGU, Washington D. C.

Pertermann, M., and M. M. Hirschmann (2003), Anhydrous partial melting experiments on MORB-like eclogite: Phase relations, phase compositions and mineral-melt partitioning of major elements at 2–3 GPa, *J. Petrol.*, *44*, 2173–2201.

Plank, T., and C. H. Langmuir (1993), Tracing trace elements from sediment input to volcanic output at subduction zones, *Nature*, *362*, 739–743.

Plank, T., and C. H. Langmuir (1998), The chemical composition of subducting sediment and its consequences for the crust and mantle, *Chem. Geol.*, *145*, 325–394.

Rapp, R. P., and E. B. Watson (1995), Dehydration melting of metabasalt at 8–32 Kbar—Implications for continental growth and crust-mantle recycling, *J. Petrol.*, *36*, 891–931.

Rapp, R. P., E. B. Watson, and C. F. Miller (1991), Partial melting of amphibolite/eclogite and the origin of Archaean trondhjemites and tonalites, *Precambrian Res.*, *51*, 1–25.

Rapp, R. P., N. Shimizu, M. D. Norman, and G. S. Applegate (1999), Reaction between slab-derived melts and peridotite in the mantle wedge: Experimental constraints at 3.8 GPa, *Chem. Geol.*, *160*, 335–356.

Richard, M., R. Maury, H. Bellon, J. F. Stephan, J. M. Boirat, and A. Calderon (1986), Geology of Mt. Iraya volcano and Batan island, northern Philippines, *Philipp. J. Volcanol.*, *3*, 1–27.

Ringwood, A. E. (1974), The petrologic evolution of island arc systems, *J. Geol. Soc. London*, *130*, 185–204.

Ringwood, A. E., and D. H. Green (1966), An experimental investigation of gabbro-eclogite transformation and some geophysical implications, *Tectonophysics*, *3*, 383–427.

Rudnick, R. L., and D. M. Fountain (1995), Nature and composition of the continental crust: A lower crustal perspective, *Rev. Geophys.*, *33*, 267–309.

Sajona, F. G., R. C. Maury, G. Prouteau, J. Cotten, P. Schiano, H. Bellon, and L. Fontaine (2000), Slab melt as metasomatic agent in island arc magma mantle sources, Negros and Batan (Philippines), *Island Arc*, *9*, 472–486.

Salters, V. J. M., J. E. Longhi, and M. Bizimis (2002), Near mantle solidus trace element partitioning at pressures up to 3.4 GPa, *Geochem. Geophys. Geosyst.*, *3*(7), 1038, doi:10.1029/2001GC000148.

Schiano, P., R. Clocchiatti, N. Shimizu, R. C. Maury, K. P. Jochum, and A. W. Hofmann (1995), Hydrous, silica-rich melts in the sub-arc mantle and their relationship with erupted arc lavas, *Nature*, *377*, 595–600.

Sharma, M., G. J. Wasserburg, D. A. Papanastassiou, J. E. Quick, E. V. Sharkov, and E. E. Lazko (1995), High Nd-143/Nd-144 in extremely depleted mantle rocks, *Earth Planet. Sci. Lett.*, *135*, 101–114.

Stalder, R., S. F. Foley, G. P. Brey, and I. Horn (1998), Mineral aqueous fluid partitioning of trace elements at 900–1200 degrees C and 3.0–5.7 GPa: New experimental data for garnet, clinopyroxene, and rutile, and implications for mantle metasomatism, *Geochim. Cosmochim. Acta*, *62*, 1781–1801.

Stalder, R., P. Ulmer, A. B. Thompson, and D. Gunther (2001), High pressure fluids in the system $MgO\text{-}SiO_2\text{–}H_2O$ under upper mantle conditions, *Contrib. Mineral. Petrol.*, *140*, 607–618.

Staudigel, H., G. R. Davies, S. R. Hart, K. M. Marchant, and B. M. Smith (1995), Large-scale isotopic Sr, Nd and O isotopic anatomy of altered oceanic crust—DSDP/ODP sites 417/418, *Earth Planet. Sci. Lett.*, *130*, 169–185.

Stolper, E. M., and S. Newman (1994), The role of water in the petrogenesis of Mariana trough magmas, *Earth Planet. Sci. Lett.*, *121*, 293–325.

Tatsumi, Y. (1981), Melting experiments on a high-magnesian andesite, *Earth Planet. Sci. Lett.*, *54*, 357–365.

Tatsumi, Y. (1982), Origin of high-magnesian andesites in the Setouchi volcanic belt, southwest Japan. II: Melting phase relations at high pressures, *Earth Planet. Sci. Lett.*, *60*, 305–317.

Tatsumi, Y., M. Sakuyama, H. Fukuyama, and I. Kushiro (1983), Generation of arc basalt magmas and thermal structure of the mantle wedge in subduction zones, *J. Geophys. Res.*, *88*, 5815–5825.

Vidal, P., C. Dupuy, R. C. Maury, and M. Richard (1989), Mantle metasomatism above subduction zones: Trace-element and radiogenic isotope characteristics of peridotite xenoliths from Batan island (Philippines), *Geology*, *17*, 1115–1118.

Wang, O., F. McDermott, J. F. Xu, H. Bellon, and Y. T. Zhu (2005), Cenozoic K-rich adakitic volcanic rocks in the Hohxil area, northern Tibet: Lower-crustal melting in an intracontinental setting, *Geology*, *33*, 465–468.

Wang, Q., Z. H. Zhao, Z. H. Bai, Z. W. Bao, X. L. Xiong, H. J. Mei, J. F. Xu, and Y. X. Wang (2003), Carboniferous adakites and Nb-enriched arc basaltic rocks association in the Alataw Mountains, north Xinjiang: Interactions between slab melt and mantle peridotite and implications for crustal growth, *Chin. Sci. Bull.*, *48*, 2108–2115.

Workman, R. K., and S. R. Hart (2005), Major and trace element composition of the depleted MORB mantle (DMM), *Earth Planet. Sci. Lett.*, *231*, 53–72.

Xiong, X. L. (2006), Trace element evidence for growth of early continental crust by melting of rutile-bearing hydrous eclogite, *Geology*, *34*, 945–948.

Yogodzinski, G. M., and P. B. Kelemen (1998), Slab melting in the Aleutians: Implications of an ion probe study of clinopyroxene in primitive adakite and basalt, *Earth Planet. Sci. Lett.*, *158*, 53–65.